J. Phys. C: Solid State Phys., Vol. 6, 1973. Printed in Great Britain.

Semiempirical calculation of deep levels: divacancy in Si†

T F Lee and T C McGill
Department of Applied Physics, California Institute of Technology, Pasadena, California 91109, USA

Received 26 March 1973, in final form 11 June 1973

Abstract. A study of the electronic levels associated with the divacancy in silicon is reported. The extended Hückel theory is shown to reproduce the band structure of silicon. The electronic levels of the divacancy are calculated by considering a periodic array of large unit cells each containing 62 atoms; a 64 atom perfect cell with two atoms removed to form the divacancy. The results are found to be in qualitative agreement with the results of EPR and infrared absorption measurements.

1. Introduction

Until recently, very little theoretical work had been reported on the difficult questions associated with deep levels in semiconductors. This lack of theoretical activity is not due to a lack of experimental information on deep levels but is due to the inherent theoretical complications thought to be associated with the deep level problem. The tightly bound character and multiplicity of charge states usually associated with deep levels make the standard effective mass theory (Kohn 1957) inappropriate. An appropriate theory of the deep electronic levels is thought to require the simultaneous accurate treatment of the potential of the defect, the lattice distortion, and the electron–electron interaction.

Previous theoretical treatments of defect levels have made use of two rather different approaches. The first pioneered by Coulson and Kearsley (1957) and extended by Coulson and Larkins (1969, 1971) makes use of the defect molecule model (DMM). In the DMM, one approximates the problem of a defect in a perfect solid by a small molecular unit consisting of the bonds near the defect. A full configuration interaction calculation is then performed on this small molecular unit. Lattice distortion is treated by expanding the energy of the defect molecule to second order in the atomic positions and minimizing this expansion to obtain the atomic positions and energy eigenvalues. While the DMM takes account of electron–electron interaction explicitly, the difficult calculations inherent in the method have prevented calculations involving more than the bonds on the nearest neighbours. Hence, the influence of bonds further away from the defect have not been included. This makes the method unsuitable for the treatment of defects where the amplitude of the wavefunction of an electronic level associated with the defect extends over more than just the nearest bonds. The DMM has been applied

† Work supported in part by Air Force Office of Scientific Research under Grant No 73-2490.

with moderate success to the vacancy in diamond by Coulson and Kearsley (1957), Coulson and Larkins (1971), and Larkins (1971a) and to the divacancy in diamond by Coulson and Larkins (1969).

Recently, Messmer and Watkins (1970) have modified the DMM so that one can treat larger molecular units. In their calculations, a finite cluster of atoms is treated using the extended Hückel theory (EHT) (Hoffman 1963). Lattice distortions are treated directly by moving atoms in the cluster about until the total energy of the system reaches a minimum. The application of the EHT to the cluster, on the one hand, makes it possible to treat very large clusters of atoms. However, on the other hand, it does not take account explicitly of the variation of electron–electron interaction and ion–ion interaction with charge state and distortion (Larkins 1971b, c).

Messmer and Watkins (1971) and Watkins and Messmer (1970) have applied these techniques with moderate success to a number of deep levels in diamond. However, Larkins (1971b, c) has shown that direct application of these methods to defects in silicon presents a number of problems. The energy gap between occupied and unoccupied levels is much larger than the band gap. The energy eigenvalues and the ordering of eigenvalues of various symmetry depend upon the size of the cluster selected.

The second approach makes use of solid state scattering theory (SST) (Callaway 1964). In this approach, the solid state continum aspects of the problem are emphasized. The defect level problem is cast in terms of the scattering of an electron off the defect potential in the presence of a perfect crystal (Bennemann 1965, Callaway and Hughes 1967). However, the method has the disadvantages that (i) it is difficult to identify the correct form of the defect potential, (ii) the treatment of lattice distortion and electron–electron interaction is hard to carry out, and (iii) a great deal of calculational work is required to obtain results.

In this paper, we report upon a study of a deep level in silicon, the divacancy. In this study we have attempted to marry some of the best points of the two methods described above. To do this, we have made calculations using the EHT for a perfect solid consisting of large unit cells with the divacancies at their centre. Hence, we have a well defined potential (the absence of two silicon atoms) and at the same time we have circumvented the difficulties associated with cluster calculations which have been noted above. Using this method we obtain results which are in qualitative agreement with known experimental results.

The outline of this paper is as follows. In § 2 we review the theoretical approach. In § 3 we report the results obtained for the silicon divacancy. § 4 contains discussions and conclusions.

2. Outline of theory

2.1. Extended Hückel theory (EHT)

In the independent electron approximation, the energy eigenvalues and eigenfunctions for a system consisting of a defect in an otherwise perfect solid are obtained by solving the time independent Schrödinger equation,

$$H\psi_i = \epsilon_i\psi_i \tag{2.1}$$

where

$$H = H_{\text{perfect}} + V_{\text{defect}}. \tag{2.2}$$

V_{defect} is defined to be the difference in potential between that found in a perfect crystal and that found with the defect present. One approach to solving (2.1) is to take ψ_i to be a linear combination of atomic orbitals, ϕ_α, centred on each atom in the crystal. That is,

$$\psi_i = \sum_\alpha C_{i\alpha}\phi_\alpha. \tag{2.3}$$

In this case, a solution to (2.1) is obtained when

$$\det |H_{\alpha\beta} - \epsilon S_{\alpha\beta}| = 0 \tag{2.4}$$

where

$$H_{\alpha\beta} = \langle \phi_\alpha | H | \phi_\beta \rangle \tag{2.5}$$

and

$$S_{\alpha\beta} = \langle \phi_\alpha | \phi_\beta \rangle. \tag{2.6}$$

In the EHT, the matrix elements of the hamiltonian between the atomic orbitals is approximated by taking

$$H_{\alpha\beta} = -\tfrac{1}{2}K_{\alpha\beta}(I_\alpha + I_\beta)S_{\alpha\beta} \qquad \text{for} \qquad \alpha \neq \beta \tag{2.7a}$$

and

$$H_{\alpha\alpha} = -I_\alpha. \tag{2.7b}$$

I_α is the empirical ionization energy of the αth atomic level and $K_{\alpha\beta}$ is a dimensionless parameter usually taken to be between 1 and 2.

2.2. Large unit cell

The method of Messmer and Watkins (1970) consists of the application of (2.4)–(2.7) to a large cluster of atoms with the defect in the centre. However, as will be discussed below, direct application of this method leads to unsatisfactory results.

To solve this problem, we have considered a perfect solid with a large unit cell. The large unit cell was chosen to consist of a cubic block of two by two by two face centred cubic cells, 32 primitive cells, or 64 atoms. This procedure ensures that a calculation for a system with no defects will give an exact energy gap.

2.3. Lattice distortion

The position of the atoms near the defect should be obtained by minimizing the total energy of the system with respect to atomic positions. The quantity in the EHT which is analogous to the total energy of the system is defined as

$$E_{\text{EHT}} = \sum_i \epsilon_i \tag{2.8}$$

where the summation runs over all the occupied states. Messmer and Watkins (1970) have used this expression for the energy to obtain the lattice distortion of the atoms in a cluster about the defect. The same process could be used with a little bit more work to calculate the lattice distortion in a large unit cell as discussed above. However, as emphasized by Larkins (1971b, c), the total energy defined by (2.8) is not precisely the total energy of the system since no explicit provision is made for taking account of electron–electron interaction, and ion–ion interaction variation with charge state and lattice distortion. Hence, minimizing (2.8) to give the equilibrium atomic positions

about the defect may give unreliable results. For this reason, we have decided to simply explore the rôle of lattice distortion on the electronic levels associated with the defect.

We will only report on one representative distortion here. The lattice distortion chosen is suggested by that deduced by Watkins and Corbett (1965) with the aid of their EPR data, see figure 1. The pairs of atoms a and c, and a' and c' are moved toward each other to improve the bonding between the 'dangling bonds' left by the removal of the

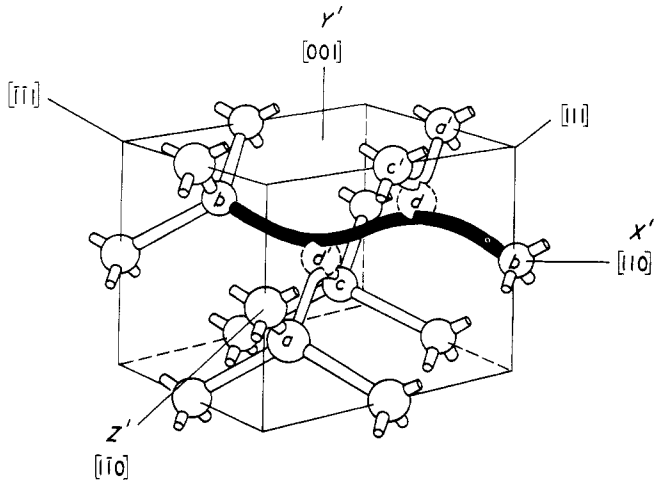

Figure 1. The model of divacancy defect in silicon deduced from EPR studies.

divacancy atoms, while the atoms b and b' are moved away from each other so that they move out of the way of the bonding pairs, ac and $a'c'$. Further, the distortion was introduced in such a way that the distortion of the bonds between the atoms next to the defect and their three nearest neighbours was confined to the stretching of a single bond and the bending of the other two bonds. If we take the location of the six nearest neighbour atoms to the divacancy in the undistorted case to be given by:

$$\boldsymbol{a} = a_0(\boldsymbol{e}_x - 3\boldsymbol{e}_y - 3\boldsymbol{e}_z)/8 \tag{2.9a}$$

$$\boldsymbol{a}' = a_0(-\boldsymbol{e}_x + 3\boldsymbol{e}_y + 3\boldsymbol{e}_z)/8 \tag{2.9b}$$

$$\boldsymbol{b} = a_0(-3\boldsymbol{e}_x - 3\boldsymbol{e}_y + \boldsymbol{e}_z)/8 \tag{2.9c}$$

$$\boldsymbol{b}' = a_0(3\boldsymbol{e}_x + 3\boldsymbol{e}_y - \boldsymbol{e}_z)/8 \tag{2.9d}$$

$$\boldsymbol{c} = a_0(-3\boldsymbol{e}_x + \boldsymbol{e}_y - 3\boldsymbol{e}_z)/8 \tag{2.9e}$$

$$\boldsymbol{c}' = a_0(3\boldsymbol{e}_x - \boldsymbol{e}_y + 3\boldsymbol{e}_z)/8. \tag{2.9f}$$

where a_0 is the length of the cube edge, then, after the distortion, the atoms are located at

$$\boldsymbol{a} = a_0[(1-\beta)\boldsymbol{e}_x - (3-\beta)\boldsymbol{e}_y - (3+\alpha)\boldsymbol{e}_z]/8 \tag{2.10a}$$

$$\boldsymbol{a}' = a_0[-(1-\beta)\boldsymbol{e}_x + (3-\beta)\boldsymbol{e}_y + (3+\alpha)\boldsymbol{e}_z]/8 \tag{2.10b}$$

$$\boldsymbol{b} = a_0[-(3+\beta)\boldsymbol{e}_x - (3+\beta)\boldsymbol{e}_y + (1+\alpha)\boldsymbol{e}_z]/8 \tag{2.10c}$$

$$\boldsymbol{b}' = a_0[(3+\beta)\boldsymbol{e}_x + (3+\beta)\boldsymbol{e}_y - (1+\alpha)\boldsymbol{e}_z]/8 \tag{2.10d}$$

$$\boldsymbol{c} = a_0[-(3-\beta)\boldsymbol{e}_x + (1-\beta)\boldsymbol{e}_y - (3+\alpha)\boldsymbol{e}_z]/8 \tag{2.10e}$$

$$\boldsymbol{c}' = a_0[(3-\beta)\boldsymbol{e}_x - (1-\beta)\boldsymbol{e}_y + (3+\alpha)\boldsymbol{e}_z]/8. \tag{2.10f}$$

α sets the scale of the distortion and

$$\beta = \left(\frac{4\alpha - \alpha^2}{2}\right)^{1/2}.$$

Distortion is measured by a parameter d defined by

$$d = \tfrac{1}{4} a_0 \sqrt{\alpha}. \tag{2.11}$$

2.4. Definition of localization

For the purpose of deciding which levels should be identified with the defect, we define a measure of localization of a level i on the six nearest neighbour atoms by:

$$P_i = \frac{\sum_{\substack{\alpha,\beta \\ \text{over six} \\ \text{atoms}}} C^*_{i\alpha} C_{i\beta} S_{\alpha\beta}}{\sum_{\substack{\alpha,\beta \\ \text{all atoms} \\ \text{unit cell}}} C^*_{i\alpha} C_{i\beta} S_{\alpha\beta}} \tag{2.12}$$

where $C_{i\alpha}$ is the αth component of eigenvector of state i.

3. Results

3.1. Silicon band structure

For suitable values of EHT parameters in (2.7), the EHT accurately reproduces the accepted band structure for silicon (Herman *et al* 1966, Messmer 1971). We have used atomic functions like those obtained by Clemente (1965). The atomic functions used differ in that we have kept only the three largest terms in the expansion in Slater orbitals and modified the Slater exponents slightly. The Slater exponents in ϕ_{3s} are increased by a factor of 1·3 and the Slater exponents in ϕ_{3p} by 1·4,

$$\phi_{3s} = [-0{\cdot}20265\,\chi_3(6{\cdot}8112, r) + 0{\cdot}61435\,\chi_3(2{\cdot}7160, r) + 0{\cdot}52025\,\chi_3(1{\cdot}6829, r)]\,Y_{0,0}(\theta, \phi) \tag{3.1}$$

and a 3p wavefunction of the form

$$\phi_{3p} = [-0{\cdot}1208\,\chi_2(9{\cdot}8, r) + 0{\cdot}48091\,\chi_4(3{\cdot}2214, r) + 0{\cdot}57523\,\chi_4(1{\cdot}8218, r)]\,Y_{1,0}(\theta, \phi) \tag{3.2}$$

where

$$\chi_n(\xi, r) = [a_B^3(2n)!]^{-1/2}\,(2\xi)^{n+\frac{1}{2}} \left(\frac{r}{a_B}\right)^{n-1} \exp(-\xi r/a_B)$$

and a_B is Bohr radius.

$$I_{3s} = 17\,\text{eV} \tag{3.3a}$$

$$I_{3p} = 11{\cdot}6\,\text{eV}. \tag{3.3b}$$

The dimensionless parameters were taken to be

$$K_{ss} = 1{\cdot}87 \tag{3.4a}$$

$$K_{pp} = 1{\cdot}81 \tag{3.4b}$$

$$K_{sp} = 1{\cdot}35. \tag{3.4c}$$

Using these parameters, we obtain the band structure shown in figure 2. The calculated value of the gap is 1·15 eV and the minimum in the conduction band occurs along the Δ direction in agreement with accepted band structures.

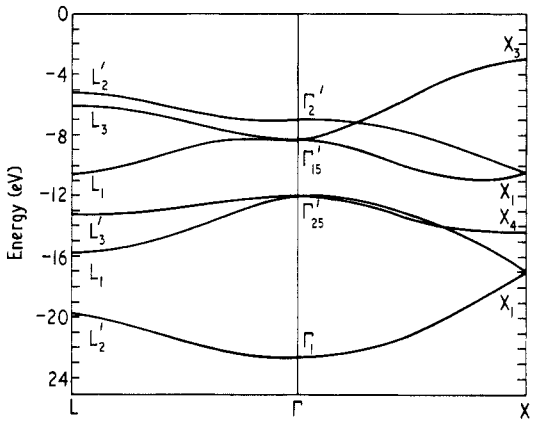

Figure 2. The band structure of silicon along Δ and Λ directions in EHT approximation. The EHT parameters: $I_{3s} = 17$, $I_{3p} = 11{\cdot}6$, $K_{ss} = 1{\cdot}87$, $K_{pp} = 1{\cdot}81$, $K_{sp} = 1{\cdot}35$. The energy gap is 1·15 eV.

3.2. Electronic levels of clusters

Calculations of the electronic levels of clusters of 29 and 64 atoms with no defect present show that energy levels of the cluster do not give a satisfactory representation of the electronic level structure for silicon. The electronic levels were calculated using the same EHT parameters as were used in the band structure calculation. The results of these calculations are shown in figure 3 where we have plotted the band structure for the large unit cell at the Γ point along with the electronic levels for the 29 and 64 atom clusters. From these results, one can see that the level structure in the cluster calculation is unlike that obtained in the band structure calculation. In this figure, we have shown the location of the energy separating occupied from unoccupied levels by an arrow. For a reasonable representation of the electronic structure of the solid, we would expect there to be a region in energy just above this arrow which would be the band gap. However, as can be easily seen from figure 3, no such gap exists for the cases of 29 atom or 64 atom cluster.

3.3. Divacancy

We will report the results for the divacancy in two parts: first the divacancy without lattice distortion; and second the divacancy with lattice distortion.

3.3.1. Undistorted. The undistorted divacancy is modelled by simply removing two atoms from the centre of each 64 atom unit cell (described in § 2.2) in a periodic structure. The

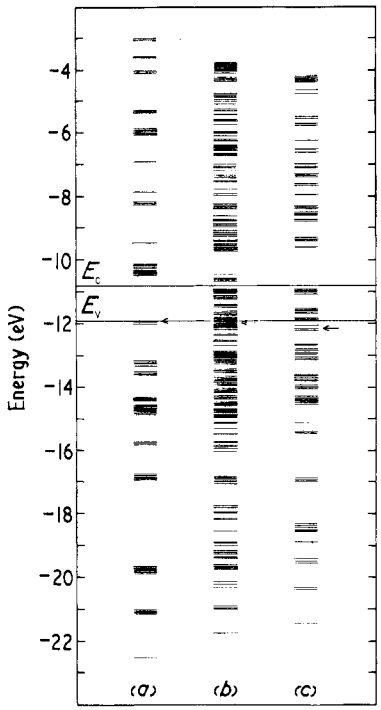

Figure 3. (*a*) The energy levels at the centre of Brillouin zone, Γ, of Si perfect crystal with 64-atom cubic unit cell. (*b*) The energy levels of 64-atom cubic silicon cluster. (*c*) The energy levels of 29-atom silicon cluster. The arrows indicate the level separating occupied from unoccupied levels in the case of a neutral unit.

resulting unit cell has symmetry D_{3d} with the 3-fold axis of symmetry along the vector connecting the positions of the atoms removed to produce the divacancy. The solid produced by this procedure consists of a periodic array of oriented divacancies at a density of approximately 10^{21} cm^{-3} in an otherwise perfect diamond lattice.

To study the electronic levels of this large unit cell, we have made calculations of the band structure at the zone centre ('Γ-point') and at the cubic Brillouin zone edge along the $(1\bar{1}0)$ direction ('M-point') oriented with respect to the divacancy as shown in figure 1. Each of our calculations yields 248 eigenvalues and eigenvectors. These 248 energy levels divide such that 125 are below the valence band edge for the perfect crystal and 123 levels are above. Hence, if we neglect dispersion in the eigenvalues in our small Brillouin zone, and the Fermi energy is at the valence band edge, then the unit cell contains two additional electrons above the four electrons per atom present when the cell is neutral.

We are interested in all the energy levels which are located in the energy gap and also those energy states which have large probabilities P around the divacancy (see (2.12)). Therefore we have plotted in figure 4 the energy levels at Γ-point and their corresponding probabilities P for all the levels in the energy gap and for the levels with P greater than 0·30. To make comparison with the results for the distorted divacancy easier, we have labelled the states with their symmetry according to C_{2h} (a subgroup of D_{3d}) (Hamermesh 1962), the symmetry of the distorted divacancy. The degeneracy of each state is indicated by the height of the line in the energy level plot. We marked in figure 4 the six most localized states by their symmetries. These six most localized states are also listed explicitly in the first series of entries in table 1. Only the six most localized states were

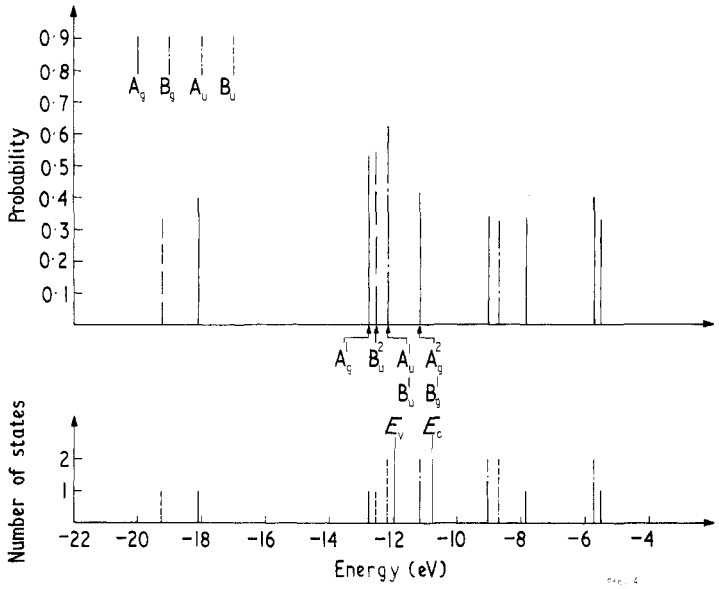

Figure 4. The energy levels of undistorted divacancy and their corresponding probabilities for all the energy states in the energy gap and the energy states with localization probabilities P greater than 0·30. The degeneracy of states is indicated by the height of the line in the energy level plot. The symmetries of the states are indicated. The six most localized states are indicated by arrows.

studied since these may be associated with the six dangling bonds around the divacancy (Watkins and Corbett 1965).

Because of the rather high density of defects ($\sim 10^{21}$ cm^{-3}) in our model, we have also investigated the rôle of defect–defect interaction. This was accomplished by computing the band structure at the above described 'M-point' and again identifying the six most highly localized states. The results of this calculation are shown in the second entry in table 1. The levels have been arranged so that they have the same symmetry as in the first entry. Comparing the two entries we see that the levels are shifted by approximately 0·2 eV and this suggests a rather strong divacancy–divacancy interaction at this density of divacancies.

To explore the use of cluster calculations which avoids the divacancy–divacancy

Table 1. The six most localized states at Γ with their corresponding states at M and the six most localized states for 62-atom cluster. The probabilities of electrons being found around the divacancy are also shown here.

Γ Symmetry	Level (eV)	Probability	M ($1\bar{1}0$) Symmetry	Level (eV)	Probability	Cluster Symmetry	Level (eV)	Probability
A_u^1	−12·19	61·9%	A_u^1	−12·0	46·8%	A_u^1	−4·4	49·8%
B_u^1	−12·19	61·9%	B_u^1	−12·1	59·6%	B_u^1	−4·4	49·8%
B_u^2	−12·53	54·0%	B_u^2	−12·43	56·3%	A_g^1	−8·37	45·0%
A_g^1	−12·79	53·0%	A_g^1	−12·55	43·3%	B_g^1	−3·8	43·5%
A_g^2	−11·6	41·5%	A_g^2	−11·96	50·2%	A_g^2	−5·14	40·8%
B_g^1	−11·6	41·5%	B_g^1	−11·81	48·5%	A_g^3	−4·8	40·0%

interaction question by use of a finite number of atoms, we have made calculations for a single divacancy centred in a cluster of 62 atoms. The resulting energy of the six most highly localized states are shown in the final entry in table 1. From these results, we see that the levels in a cluster calculation bear little resemblance in location and symmetry to those obtained in the above-described calculation.

3.3.2. Distorted. The introduction of the lattice distortion discussed in § 2.3 lowers the symmetry about the divacancy from D_{3d} to C_{2h} (Watkins and Corbett 1965). We have studied the influence of this lattice distortion on the energy and degree of localization of the six most highly localized levels. In figures 5 and 6 we have plotted the energy and

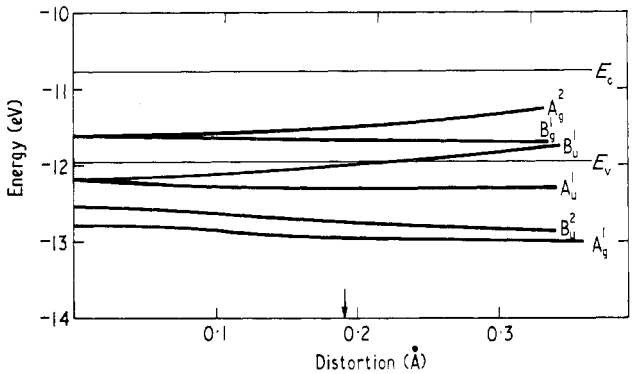

Figure 5. The variation of the six localized states as a function of distortion.

probability of being on the six nearest neighbour atoms, respectively, as a function of the lattice distortion measured by d (see equation 2.11). From these figures we see that: (i) the energy of highly localized B_u^1 moves from the valence band into the energy gap; (ii) the state A_g^2 increases in energy but remains in the energy gap for reasonable values of

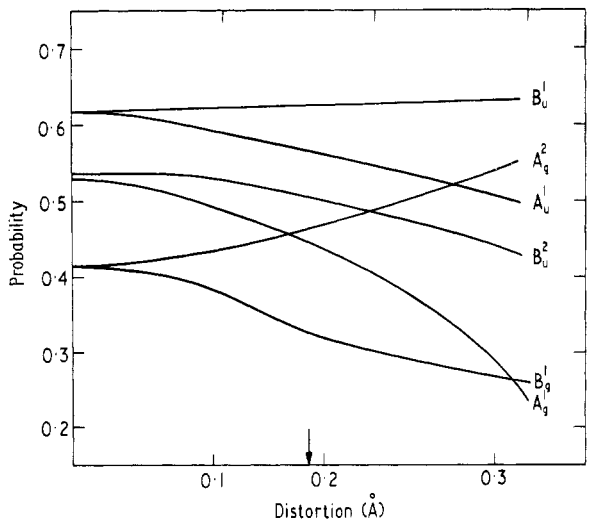

Figure 6. The probabilities of the six localized states around the six nearest atoms to divacancy.

the distortion, and becomes more highly localized; (iii) the energy of the state with symmetry B_g^1 remains in the energy gap but becomes more diffuse.

Turning our attention to the three states in the energy gap, the state with symmetry B_g^1 is localized around the four atoms a, d, and a', d' (see figure 1 for labelling of atoms around defect). The states A_g^2 and B_u^1 are localized largely on the two atoms b and b'. The best agreement between these energy eigenvalues and the experimental observed properties of the divacancy (see § 4) is obtained when the distortion is 0·19 Å (Watkins 1968). For the case in which the divacancy is distorted by 0·19 Å, we have plotted in figure 7 the energy levels and the corresponding probabilities P for all the states in the energy gap

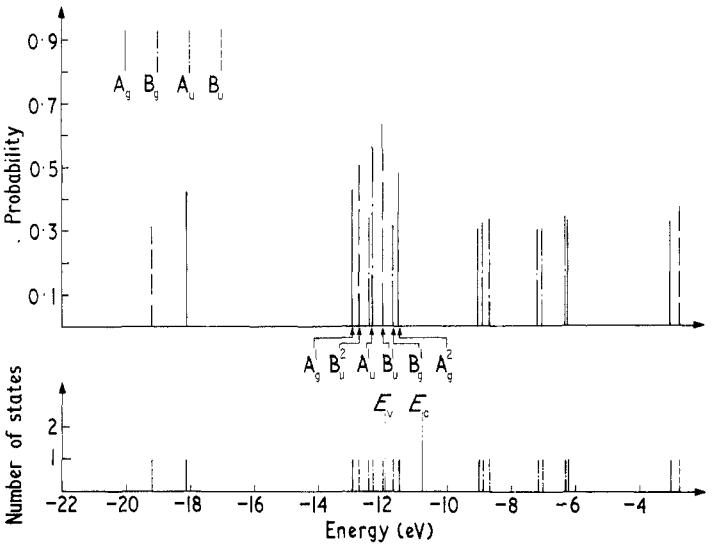

Figure 7. The energy levels of distorted divacancy and their corresponding probabilities for all the energy states in the energy gap and the energy states with localization probabilities P greater than 0·30. The symmetries of the states are indicated. The six states which are thought to be associated with the dangling bonds of divacancy are indicated by arrows.

and for the states with probabilities greater than 0·30. The symmetries of the states are indicated by using different symbols for different symmetries. The six states which are thought to be associated with the dangling bonds of divacancy are marked by their symmetries in figure 7. As we can see, most of the highly localized states are either in the energy gap or close to the top of the valence band.

For this value of the distortion, the 248 energy levels divide such that 124 levels are below the band edge for the perfect crystal and 124 levels are above. Hence, if we neglect dispersion in the eigenvalues in our small Brillouin zone, and the Fermi energy is at the valence band edge, then the unit cell contains four electrons per atom and is neutral.

To estimate the size of divacancy–divacancy interactions, we have also calculated the energy levels at the 'M point' (see definition given above) and at the zone boundary along $(1\bar{1}1)$ direction, 'R point'. The results of this calculation along with the values at the Γ point for $d = 0{\cdot}19$ Å are given in table 2. As in the results for the undistorted divacancy, we note that divacancy–divacancy interaction at this density can produce level shifts which are of the order of 0·2 eV. We also note that at 'R point' the B_g^1 level is in valence band and the A_g^2 and B_u^1 levels are in the energy gap. Therefore the presence of the

Table 2. The six localized states at zone centre Γ and zone edge M and R when atoms deviate 0·19 Å from their original sites.

Γ Symmetry	Level (eV)	Probability	M ($1\bar{1}0$) Symmetry	Level (eV)	Probability	R ($1\bar{1}1$) Symmetry	Level (eV)	Probability
B_u^1	−11·98	63·3%	B_u^1	−11·97	62·1%	B_u^1	−11·86	56·0%
A_u^1	−12·32	55·8%	A_u^1	−12·13	31·4%	A_u^1	−12·2	44·6%
B_u^2	−12·75	50·6%	B_u^2	−12·62	50·6%	B_u^2	−12·9	40·8%
A_g^2	−11·49	47·9%	A_g^2	−11·7	56·8%	A_g^2	−11·7	59·0%
A_g^1	−12·95	42·5%	A_g^1	−12·93	45·1%	A_g^1	−12·7	33·9%
B_g^1	−11·69	31·6%	B_g^1	−11·88	42·1%	B_g^1	−12·0	51·0%

B_g^1 level in the energy gap is uncertain; it may be due to divacancy–divacancy interactions or due to only six nearest atoms to divacancy being distorted.

4. Discussion and conclusions

Using the extended Hückel theory (EHT), we calculated the band structure of silicon. The calculated band structure is in good agreement with the accepted band structure for silicon showing that EHT is capable of reproducing the band structure of silicon.

Calculations of the electronic levels of free clusters of 29 and 64 atoms spatially arranged as in a perfect diamond lattice show that the electronic structure of the clusters is not the same as that of the perfect solid. If we define the top of the valence band as that energy below which half of the electronic levels occur, then the energy range from the top of the valence band to that energy plus the band gap is filled almost completely by electronic levels. This fact has necessitated our use of the large unit cell.

Using the parameters obtained in the band structure calculation, we have calculated the electronic levels for the distorted and undistorted divacancy. Labelling all the states by their symmetry in the case of the distorted divacancy, we find that the six states most highly localized about the divacancy, listed in table 1, have the same symmetry and ordering as the six molecular states in the LCAO model proposed by Watkins and Corbett (1965). In the results presented here, the states with symmetries A_g^2 and B_g^1 are in the band gap while the remaining four states are in the valence band.

Distortion is introduced by simply moving the atoms nearest the divacancy in such a way that the symmetry around the defect is C_{2h}. This distortion produces changes in the energy of the divacancy as well as changes in the degree of localization of the states about the defect. While the distortion is very much like that envisaged by Watkins and Corbett (1965) the ordering of the states after distortion is different from that of the LCAO molecular orbital results. This result is due to interaction between the divacancy levels and the conduction or valence bands. After distortion the A_g^2 level is still inside the band gap, and the B_u^1 level has moved up into the gap; the B_g^1 level moves downwards. The position of the B_g^1 level is uncertain since due to its more diffuse nature it is subject to greater influence by divacancy–divacancy interaction and distortion of the atoms away from the defect than the other levels. A calculation which takes account of these factors may locate the B_g^1 level in the valence band.

The results of these divacancy calculations are consistent with the experimental results at present available. The EPR studies of Watkins and Corbett (1965) have identified

two spectral features labelled Si-G6 and Si-G7. Study of the hyperfine interactions in these spectral features has led them to conclude that about 50–60% of the total probability for an electron contributing to the EPR are localized about atoms b and b' in figure 1 and about 10–15% of this probability is S-like.

We interpret the Si-G6 and Si-G7 spectra as arising from single occupancy of the B_u^1, and A_g^2 levels, respectively. These two levels are in or near the band gap depending upon the degree of distortion; and 40–50% of the probabilities are found about the b and b' atoms. Furthermore, when the divacancy is distorted to equal 0·19 Å (see equation 2.11), the S-wave character of the states about b and b' is about 10–15%. Both of these qualities are in reasonable agreement with the experimentally determined values.

Studies have also been made of the infrared absorption (Fan *et al* 1959, Vavilov *et al* 1963, Corelli *et al* 1965, Cheng *et al* 1966, Young *et al* 1969, Chen and Corelli 1972) and photoconductivity (Cheng 1967, 1968, Kalma and Corelli 1968, Young and Corelli 1972) of samples containing divacancies. While there seems to be a number of contradictory experimental results, there does seem to be a 1·8 μm (0·69 eV) absorption in the infrared. Experiments suggest that this absorption is due to highly localized states on the negatively charged divacancy. Group theoretical arguments suggest that this transition is between states having A_g and B_u symmetry or between states having A_u and B_g symmetry. Our theoretical calculation suggests that the transition is between our A_g^2 and B_u^1 states. The calculated energy difference is 0·5 eV, which is reasonable agreement with the 0·69 eV observed. We have been unable to identify the number of other transitions reported by various authors.

In conclusion, the extended Hückel theory combined with periodic boundary conditions induced by using a large unit cell gives results in qualitative agreement with the experimental results available.

Acknowledgment

The authors would like to acknowledge discussions with R P Messmer, G D Watkins, and F P Larkins.

References

Bennemann K H 1965 *Phys. Rev.* **137** A1497–514
Callaway J 1964 *J. math. Phys.* **5** 783–98
Callaway J and Hughes A J 1967 *Phys. Rev.* **164** 1043–9
Chem C S and Corelli J C 1972 *Phys. Rev.* B **5** 1505–17
Cheng L J 1967 *Phys. Lett.* **24A** 729–31
—— 1968 in *Radiation Effects in Semiconductors* ed F L Vook (New York: Plenum) 143–51
Cheng L J, Corelli J C, Corbett J W, and Watkins G D 1966 *Phys. Rev.* **152** 761–74
Clementi E 1965 *Suppl IBM J. Res. Dev.* **9** 2 Table 01–06
Corelli J C, Oehler G, Becker J F, and Eisentraut K J 1965 *J. appl. Phys.* **36** 1787–8
Coulson C A and Kearsley M J 1957 *Proc. R. Soc.* A **241** 433–53
Coulson C A and Larkins F P 1969 *J. Phys. Chem. Solids* **30** 1963–72
—— 1971 *J. Phys. Chem. Solids* **32** 2245–57
Fan H Y and Ramadas A K 1959 *J. appl. Phys.* **30** 1127–34
Hamermesh W 1962 *Group Theory and Its Application to Physical Problems* (New York: Addison Wesley) 125–6
Herman F *et al* 1966 *Quantum Theory of Atoms, Molecules, and the Solid State* ed P Lowdin (New York: Academic Press) 381–428

Hoffman R 1963 *J. chem. Phys.* **39** 1397–412
Kalma A H and Corelli J C 1968 *Phys. Rev.* **173** 734–45
Kohn W 1957 *Solid State Phys.* eds F Seitz and D Turnbull (New York: Academic Press) **5** 257–320
Larkins F P 1971a *J. Phys. Chem. Solids* **32** 2123–8
—— 1971b *J. Phys. Chem. Solids* **4** 3065–76
—— 1971c *J. Phys. Chem. Solids* **4** 3077–82
Messmer R P 1971 *Chem. Phys. Lett.* **11** 589–92
Messmer R P and Watkins G D 1970 *Phys. Rev. Lett.* **25** 656–9
—— 1971 *Radiation Effects* **9** 9–14
Vavilov V S, Plotnikov A F, and Tkachev V D 1963 *Sov. Phys.–Solid St.* **4** 2522–8
Watkins G D 1968 *Radiation Effects in Semiconductors* ed F L Vook (New York: Plenum) 67–81
Watkins G D and Corbett J W 1965 *Phys. Rev.* **138** A543–55
Watkins G D and Messmer R P 1970 *Proc. Tenth Int. Conf. on the Physics of Semiconductors, Cambridge, Mass.* eds S P Keller, J C Hensel and F Stern (Oak Ridge, Tennessee: USAEC) 623–7
Young R C and Corelli J C 1972 *Phys. Rev.* B **5** 1455–67
Young R C, Westhead J W and Corelli J C 1969 *J. appl. Phys.* **40** 271–8